

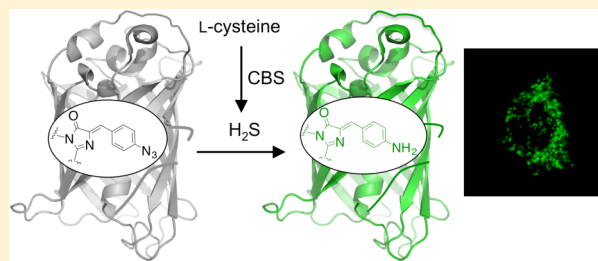
# A Highly Responsive and Selective Fluorescent Probe for Imaging Physiological Hydrogen Sulfide

Zhi-jie Chen and Hui-wang Ai\*

Department of Chemistry, University of California, 501 Big Springs Road, Riverside, California 92521, United States

**S** Supporting Information

**ABSTRACT:** The discovery of hydrogen sulfide ( $\text{H}_2\text{S}$ ) as a novel gasotransmitter for cell signaling and other pathophysiological processes has spurred tremendous interest in developing analytical methods for its detection in biological systems. Herein, we report the development of a highly responsive and selective genetically encoded  $\text{H}_2\text{S}$  probe, hsGFP, for the detection of  $\text{H}_2\text{S}$  both *in vitro* and in living mammalian cells. hsGFP bestows a combination of favorable properties, including large fluorescence responses, high efficiency in folding and chromophore formation, and excellent sensitivity and selectivity toward  $\text{H}_2\text{S}$ . As a genetically encoded probe, hsGFP can be readily and precisely localized to subcellular domains such as mitochondria, cell nuclei, and ion channels. hsGFP was further utilized to image  $\text{H}_2\text{S}$  enzymatically produced from L-cysteine in human embryonic kidney (HEK) 293T cells.



Hydrogen sulfide ( $\text{H}_2\text{S}$ ), a gaseous molecule with the unique foul odor of rotten eggs, has long been regarded as a toxicant.<sup>1</sup> Naturally,  $\text{H}_2\text{S}$  is primarily produced from geological activities such as volcanic eruptions and from microbial breakdown of organic matter.<sup>2,3</sup> The major enzymatic sources of  $\text{H}_2\text{S}$  production in mammals are cystathionine  $\beta$ -synthase (CBS), cystathionine  $\gamma$ -lyase (CSE), and 3-mercaptopyruvate sulfurtransferase (3-MST).<sup>4</sup> In recent years, emerging evidence has suggested that  $\text{H}_2\text{S}$  also serves as an important gasotransmitter in biological systems.<sup>4–7</sup>  $\text{H}_2\text{S}$  has been shown to participate in the post-translational modification of protein cysteine residues, leading to S-sulfhydration.<sup>8,9</sup>  $\text{H}_2\text{S}$  also acts as a relaxant of smooth muscle and a regulator of cardiovascular and gastrointestinal systems.<sup>10,11</sup> In addition,  $\text{H}_2\text{S}$  has been reported to modulate ATP-sensitive potassium ( $\text{K}_{\text{ATP}}$ ) channels and some other potassium channels.<sup>12</sup> Aberrant production of  $\text{H}_2\text{S}$  has been linked to serious pathological consequences, such as Alzheimer's disease,<sup>13</sup> Down syndrome,<sup>14</sup> diabetes,<sup>15</sup> hypertension,<sup>16</sup> and liver cirrhosis.<sup>17</sup> There is thus a need to dissect the production, diffusion, signaling, and turnover of  $\text{H}_2\text{S}$  in biological systems, using noninvasive detection methods.<sup>18,19</sup>

The detection of  $\text{H}_2\text{S}$ , a prerequisite for understanding its diverse physiological and pathological roles, has long been challenging. Recently, a group of  $\text{H}_2\text{S}$ -responsive fluorescent probes have been developed to partially relieve these problems. In particular, copper sulfide precipitation,<sup>20–22</sup>  $\text{H}_2\text{S}$  trapping via nucleophilic addition,<sup>23–25</sup> and  $\text{H}_2\text{S}$ -mediated reduction of azides to amines<sup>26–30</sup> are examples of the most successful and prevailing strategies for designing  $\text{H}_2\text{S}$ -reactive probes. While the ever-expanding set of synthetic  $\text{H}_2\text{S}$  probes is gaining increasing popularity, numerous technical obstacles remain to be overcome. A diffusion-controlled delivery of synthetic  $\text{H}_2\text{S}$  probes is unlikely to localize the dyes to a specific subtype of cells or tissues where  $\text{H}_2\text{S}$  signaling events actually occur.

Within a single cell, it is not straightforward to target synthetic  $\text{H}_2\text{S}$  probes to subcellular domains to measure the generation, transport, and concentration of subcellular  $\text{H}_2\text{S}$ . Even though certain functional groups can be utilized to derivatize these chemical probes and lead them to subcellular domains, these strategies have proven to be challenging and laborious.<sup>31</sup> To date, only very few  $\text{H}_2\text{S}$  probes have been reported to be capable of mitochondrial and lysosomal localization in mammalian cells.<sup>32,33</sup>

We previously reported a genetically encoded fluorescent probe for  $\text{H}_2\text{S}$ ,<sup>34</sup> which has the potential to address some of the aforementioned problems. A genetic code expansion technology<sup>35,36</sup> was used to introduce the unnatural amino acid (UAA), *p*-azidophenylalanine (*p*AzF), into a circularly permuted green fluorescent protein (cpGFP), thereby generating the first genetically encoded fluorescent  $\text{H}_2\text{S}$  sensor, cpGFP-*p*AzF. It reacts with  $\text{H}_2\text{S}$  to form a fluorescent *p*-aminobenzylideneimidazolidone chromophore. However, this proof-of-concept sensor suffers from poor sensitivity and a low signal-to-noise ratio. Only an  $\sim 60\%$  increase in fluorescence in response to  $100\ \mu\text{M}$   $\text{H}_2\text{S}$  was observed. The use of this sensor to detect small amounts of biologically generated  $\text{H}_2\text{S}$  is thus technically challenging and may even be impractical.

Herein, we present our recent efforts in engineering a significantly enhanced, genetically encoded fluorescent  $\text{H}_2\text{S}$  probe, hsGFP. hsGFP has a large dynamic range, high specificity for  $\text{H}_2\text{S}$  over other cellular redox signaling molecules, and an ability to efficiently fold and form the mature chromophore. These properties effectively allowed the use of

Received: July 7, 2014

Revised: August 19, 2014

Published: August 20, 2014



hsGFP to sensitively and selectively detect  $\text{H}_2\text{S}$  *in vitro* and in living cells. We also show that hsGFP can be easily targeted to subcellular domains, including mitochondria, cell nuclei, and  $\text{K}_{\text{ATP}}$  channels, to efficiently respond to  $\text{H}_2\text{S}$ . Moreover, hsGFP can also be used to image enzymatically produced  $\text{H}_2\text{S}$  in HEK 293T cells. hsGFP is a highly robust genetic reporter for  $\text{H}_2\text{S}$  that has opened new doors for dissecting the complex roles of  $\text{H}_2\text{S}$  under diverse physiological and pathological conditions.

## MATERIALS AND METHODS

**Materials and General Methods.** Plasmids pSUR1-EYFP and pcDNA3.1-Kir6.2-GFP encoding  $\text{K}_{\text{ATP}}$  channels were kindly provided by C. Nichols (Washington University in St. Louis, St. Louis, MO).<sup>37</sup> Other materials were acquired and general procedures were performed as previously described.<sup>34,38</sup> Sodium hydrosulfide (NaSH) in phosphate-buffered saline (PBS) (pH 7.4) was employed as the  $\text{H}_2\text{S}$  donor throughout this work.

**Library Screening.** Previously, to engineer a selective peroxynitrite ( $\text{ONOO}^-$ ) probe, a superfolder GFP was utilized as the starting gene template to create a library of circularly permuted variants with randomized N- and C-termini.<sup>38</sup> The same library was utilized to screen for mutants that responded to  $\text{H}_2\text{S}$ . Briefly, the gene library in the pBAD/His B plasmid was used to cotransform *Escherichia coli* DH10B competent cells with pEvol-pAzF by electroporation.<sup>39,40</sup> Cells were grown on Luria-Bertani (LB) broth agar plates supplemented with 100  $\mu\text{g}/\text{mL}$  ampicillin, 50  $\mu\text{g}/\text{mL}$  chloramphenicol, 0.04% L-arabinose, and 1 mM pAzF. LB agar plates were incubated at 37 °C for 36 h. Subsequently, 5 mM NaHS in PBS (pH 7.4) was sprayed three times prior to selecting highly fluorescent colonies. Between each spray, plates were left at room temperature for 1 h. Selected colonies were grown in liquid LB medium and induced with 0.04% L-arabinose for protein expression. Crude proteins were extracted with B-PER Bacterial Protein Extraction Reagents (Pierce, Rockford, IL). NaHS in PBS (pH 7.4) was added to the crude mixtures for a final concentration of 1 mM, and the fluorescence responses were monitored using a Synergy Mx Microplate Reader (BioTek, Winooski, VT).

**Protein Expression and Purification.** To express hsGFP, DH10B cells were cotransformed with pEvol-pAzF and pBAD-hsGFP by electroporation and grown on LB agar containing 100  $\mu\text{g}/\text{mL}$  ampicillin and 50  $\mu\text{g}/\text{mL}$  chloramphenicol at 37 °C overnight. A single colony was grown in a starter culture of 5 mL of LB broth with appropriate antibiotics at 37 °C and 220 rpm overnight. A saturated starter culture was diluted 100-fold into terrific broth (TB) medium containing the appropriate antibiotics and grown under the same conditions. When the  $\text{OD}_{600}$  reached 0.8, the expression culture was induced with 0.2% L-arabinose and 1 mM pAzF. Culture flasks were wrapped with aluminum foil to prevent the light deactivation of pAzF. Cells continued to grow under the same conditions for 24 h and then in a shaking 30 °C water bath for an additional 24 h. Cells were then harvested and lysed. The hexa-His-tagged hsGFP protein was affinity-purified with nickel-nitrilotriacetic acid (Ni-NTA) agarose beads under native conditions as previously described.<sup>38</sup> The protein was concentrated and buffer-exchanged into 1× PBS using a 3K molecular weight cutoff Amicon Ultra centrifugal filter (Millipore, Billerica, MA). Its concentration was determined with a Bradford assay in comparison to a series of bovine serum albumin (BSA) standards.

**In Vitro Characterization.** A final protein concentration of 0.5  $\mu\text{M}$  was used for *in vitro* assays as previously described.<sup>38</sup> All assays were performed in 1× PBS (pH 7.4) at room temperature. Absorption, fluorescence excitation, and fluorescence emission spectra were recorded before and after exposure of hsGFP to 5 mM NaSH in PBS (pH 7.4) for 30 min. Fluorescence kinetics assays were performed by measuring the point fluorescence (excitation at 460 nm, emission at 500 nm) over 30 min at 2 min intervals. Fluorescent responses of hsGFP to  $\text{H}_2\text{S}$  at low micromolar concentrations were spurred by mixing 0.5  $\mu\text{M}$  hsGFP protein with the indicated concentrations of  $\text{H}_2\text{S}$  for 1 h at room temperature. Data points were represented as averages from three independent measurements  $\pm$  the standard deviation (SD). Fluorescence intensities were normalized to a control group with addition of PBS. A linear calibration curve ( $y = 0.097x + 1.0155$ ;  $R^2 = 0.979$ ) was obtained. The SD of the intercept and the slope (S) of the curve were used to calculate the limit of detection (LOD) as  $3.3(\text{SD}/\text{S})$ . Selectivity assays were performed by incubating hsGFP with various redox-active molecules for 20 min at room temperature. Fluorescence intensities at 500 nm were quantified and represented as means  $\pm$  SD from three independent measurements.

**Comparison of hsGFP and cpGFP-pAzF in *E. coli*.** *E. coli* cells were treated in parallel to express either cpGFP-pAzF or hsGFP. Cells were pelleted, washed three times with PBS, and next resuspended in PBS with the  $\text{OD}_{600}$  adjusted to 0.8.  $\text{H}_2\text{S}$  (200  $\mu\text{M}$ ) was added, and the mixture was incubated for 1 h at room temperature. Fluorescence intensities at 500 nm with a 460 nm excitation were quantified. Data are means  $\pm$  SD from three independent measurements.

**Construction of Mammalian Expression Plasmids.** The hsGFP gene in pBAD was amplified with oligonucleotides pCMV-hsGFP-F-HindIII and pCMV-hsGFP-R-XhoI (see Table S1 of the Supporting Information). After digestion with HindIII and XhoI, the product was ligated into a predigested pcDNA3-pnGFP plasmid,<sup>38</sup> resulting in pcDNA3-hsGFP for the mammalian expression of hsGFP. To construct pMito-hsGFP for mitochondrial matrix localization, a mitochondrial localization sequence (MLSRLQSIKFFKPATRTLC-SSRYLL) derived from cytochrome oxidase subunit IV was appended to the N-terminus of hsGFP using an overlap extension polymerase chain reaction (PCR) strategy with oligonucleotides pCMV-Mito-1F, pCMV-Mito-2F, pCMV-Mito-3F, and pCMV-hsGFP-R-XhoI. To construct phsGFP-Nuc for the nuclear localization of hsGFP, pCMV-Nuc-F-NheI and pCMV-Nuc-R-XhoI were utilized to amplify hsGFP. The PCR product was digested with NheI and XhoI and ligated into a predigested pEYFP-Nuc plasmid (Clontech). To construct pSUR1-Kir6.2-hsGFP for the localization of hsGFP to  $\text{K}_{\text{ATP}}$  ion channels, pCMV-SUR1-F-EcoRI and pCMV-SUR1-R-AgeI were utilized to amplify SUR1 (sulfonyleurea receptor) from pSUR1-EYFP. Oligonucleotides Kir6.2-F-AgeI, Kir6.2-R-hsGFP, Kir6.2-F-hsGFP, and pCMV-hsGFP-R-XhoI were used to amplify the Kir6.2  $\text{K}_{\text{ATP}}$  channel gene from pcDNA3.1-Kir6.2-GFP and the hsGFP gene from the pBAD plasmid. The Kir6.2 and hsGFP genes were fused in a second-step overlap extension PCR. The two DNA fragments containing genes for SUR1, or Kir6.2 and hsGFP, were digested with EcoRI and AgeI, or AgeI and XhoI, respectively. A three-part ligation reaction was conducted to ligate the two digested pieces into a pcDNA3 vector treated with EcoRI and XhoI. The human CBS gene was requested from the DNASU

cpGFP- <i>pAzF</i>	MGSAGYNSTNVYITADKQKNGIKANFKIRHNIEDGGVQLADHYQONTPIGDGPVLLPDNH
pnGFP	MGSS <sup>N<sub>1</sub>L<sub>145</sub></sup> TYNSHKVYITADKQKNGIKVNFKIRHNVEDGSGVQLADHYQONTPIGDGPVLLPDNH
hsGFP	MGSS <sup>N<sub>1</sub>L<sub>145</sub></sup> TYNSHKVYITADKQKNGIKVNFKIRHNVEDGSGVQLADHYQONTPIGDGPVLLPDNH
cpGFP- <i>pAzF</i>	YLSFQSALS <sup>201</sup> KDPNEKRDH <sup>211</sup> MLLEFVTAAGIT <sup>221</sup> LGMD <sup>231</sup> ELYK <sup>238</sup> VDGGSGGTG <sup>11</sup> YSKGEELFTGVV
pnGFP	YLSTQSVLSKDPNEKRDH <sup>201</sup> MLLEFVTAAGIT <sup>211</sup> LGMD <sup>221</sup> ELYK <sup>231</sup> VDGGSGGTG <sup>238</sup> VSKGEELFTGVV
hsGFP	YLSTQSVLSKDPNEKRDH <sup>201</sup> MLLEFVTAAGIT <sup>211</sup> LGMD <sup>221</sup> ELYK <sup>231</sup> VDGGSGGTG <sup>238</sup> VSKGEELFTGVV
cpGFP- <i>pAzF</i>	PILVELDGDVNGHKFSVSGEGEGDATY <sup>21</sup> GKLTLK <sup>31</sup> LICTTGKLPVPWPTLV <sup>41</sup> TTF <sup>51</sup> GZGLK <sup>61</sup> CFA
pnGFP	PILVELDGDVNGHKFSVSGEGEGDATNGKLT <sup>21</sup> LK <sup>31</sup> FICTTGKLPVPWPTLV <sup>41</sup> TTLT <sup>51</sup> GVQCFS
hsGFP	PILVELDGDVNGHKFSVSGEGEGDATNGKLT <sup>21</sup> LK <sup>31</sup> FICTTGKLPVPWPTLV <sup>41</sup> TTLT <sup>51</sup> GVQCFS
cpGFP- <i>pAzF</i>	RYPDHMKQHDFFKSAMPEGYVQERTIFFKDDGNYKTRA <sup>81</sup> EVKFE <sup>91</sup> GD <sup>101</sup> TLVNRIELK <sup>111</sup> GIDFKE
pnGFP	RYPDHMKQHDFFKSAMPEGYVQERTIFFKDDGTYKTRA <sup>81</sup> EVKFE <sup>91</sup> GD <sup>101</sup> TLVNRIELK <sup>111</sup> GIDFKE
hsGFP	RYPDHMKQHDFFKSAMPEGYVQERTIFFKDDGTYKTRA <sup>81</sup> EVKFE <sup>91</sup> GD <sup>101</sup> TLVNRIELK <sup>111</sup> GIDFKE
cpGFP- <i>pAzF</i>	DGNILGHKLEYN <sup>141</sup> GT <sup>144</sup> TD----
pnGFP	DGNILGHKLEYN <sup>141</sup> THHHHHH
hsGFP	DGNILGHKLEYN <sup>141</sup> WHHHHHH

**Figure 1.** Sequence alignment of hsGFP and several other genetically encoded probes for H<sub>2</sub>S and ONOO<sup>−</sup>. Residues forming the chromophores are boxed in green. *pAzF* and *pBoF* are shown as Z and B, respectively (colored magenta). The N- and C-terminal mutations of hsGFP are colored blue. Residues are numbered according to the sequence of wild-type GFP.

plasmid repository (Clone ID HsCD00002251) and cloned into pcDNA3 using two oligonucleotides, pCMV-CBS-F and pCMV-CBS-R.

**Mammalian Cell Culture and Imaging.** Culturing, transfection, and imaging of HEK 293T cells was performed as previously described.<sup>38</sup> After transfection, cells were cultured in complete medium containing 1 mM *pAzF* for 48 h. Cells were further cultured in fresh complete medium without *pAzF* for an additional 12 h to deplete free *pAzF*. Time-lapse imaging experiments were performed by incubating cells with 50 μM H<sub>2</sub>S buffered in PBS (pH 7.4). Images were taken every 30 s for a total duration of 40 min. Fluorescence images of hsGFP at subcellular domains were taken after incubating the cells with 100 μM buffered H<sub>2</sub>S at 37 °C for 1 h in Dulbecco's PBS (DPBS). To stimulate the enzymatic production of H<sub>2</sub>S in HEK 293T cells, cells were incubated in DPBS containing 1 mM L-cysteine at 37 °C for 3 h. Before being imaged, cells were washed twice with DPBS containing 1 mM Ca<sup>2+</sup> and 1 mM Mg<sup>2+</sup>. Next, cells in DPBS were imaged under either a Leica SP2 or a Leica SP5 confocal fluorescence microscope at the microscopy core of the UCR Institute for Integrative Genome Biology. The excitation laser was set at 488 nm, and emission was collected between 500 and 600 nm. The airy unit of the pinhole was set to 1.

## RESULTS AND DISCUSSION

**Laboratory Engineering of hsGFP.** The first genetically encoded H<sub>2</sub>S probe, cpGFP-*pAzF*, was derived by replacing Tyr66 of a cpGFP with *pAzF* using a genetic code expansion technology (Figure 1).<sup>34</sup> Its fluorescence responded to H<sub>2</sub>S at a small magnitude. The formation of a *pAzF*-derived mature chromophore was also disfavored, via observation of a large percentage of ribosomally synthesized peptides without undertaking chromophore maturation reactions. Even though this proof-of-concept probe has previously been demonstrated to be capable of detecting H<sub>2</sub>S *in vitro* and in live cells, broader applications require a more robust probe.

We recently also developed a fluorescent probe pnGFP for the detection of peroxynitrite (ONOO<sup>−</sup>).<sup>38</sup> We circularly permuted a superfolder GFP.<sup>41</sup> The new N- and C-terminal

amino acid residues were fully randomized, and the resulting library was screened for selective responses to ONOO<sup>−</sup>. The probe pnGFP was identified to show a large fluorescence enhancement in response to ONOO<sup>−</sup> *in vitro* and in live cells. pnGFP is also efficient in protein folding and chromophore maturation. We reasoned that these favorable properties of pnGFP are likely associated with the new superfolder GFP template, so we hypothesized that *pAzF* could also be introduced into this new template to derive H<sub>2</sub>S sensors with improved properties to achieve a sensitive detection of H<sub>2</sub>S. To test this notion, we screened the same library used to derive pnGFP, but for H<sub>2</sub>S-induced fluorescence changes (Figure 2).

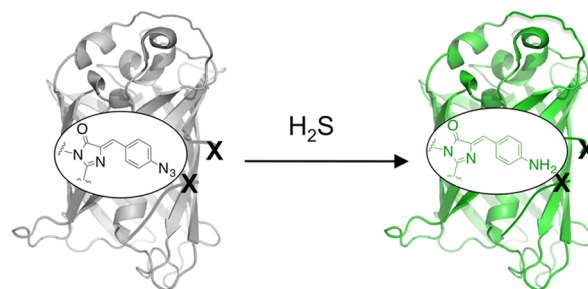


**Figure 2.** Schematic representation of hsGFP activation. The original N- and C-termini of superfolder GFP were connected with a floppy peptide linker. The new N- and C-termini were fully randomized and screened for H<sub>2</sub>S-induced fluorescence changes. The chemical structures of the chromophore before and after conversion are also shown. The basic tertiary structure schematic was adapted from Protein Data Bank entry 2B3P.

*pAzF* was utilized to replace *p*-boronophenylalanine (*pBoF*) in pnGFP to synthesize *pAzF*-containing proteins in bacterial colonies. These bacterial colonies were challenged with H<sub>2</sub>S. We first selected highly fluorescent colonies after reaction with H<sub>2</sub>S. Next, we cultured these colonies in liquid media for protein expression. Crude proteins were prepared and used for secondary screening. Their fluorescence intensities before and after reaction with H<sub>2</sub>S were quantitatively measured. At this stage, the ratio of the two intensities was used as our selection



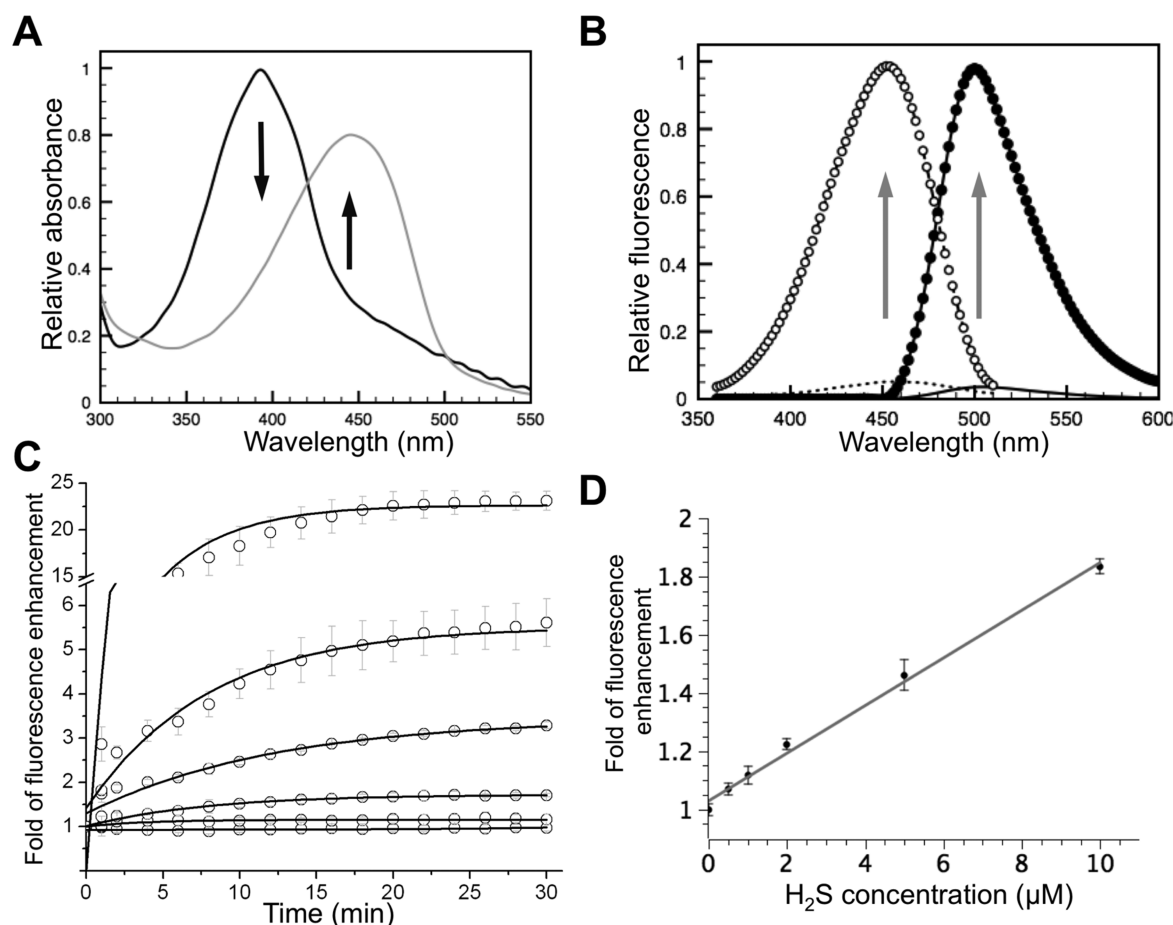


**Figure 3.** Spectroscopic responses of hsGFP to H<sub>2</sub>S. (A) Absorption spectra of hsGFP before (black) and after (gray) 5 mM H<sub>2</sub>S treatment, with arrows indicating an absorbance decrease at ~391 nm and a concomitant increase at ~452 nm upon addition of H<sub>2</sub>S. (B) Excitation and emission spectra of hsGFP before and after a 5 mM H<sub>2</sub>S treatment, with arrows indicating the increase in excitation and emission at ~454 and ~500 nm, respectively. (C) Fluorescence changes of hsGFP (0.5 μM) in response to various concentrations of H<sub>2</sub>S (H<sub>2</sub>S concentrations are 1 mM, 100 μM, 50 μM, 10 μM, 1 μM, and 0 μM from top to bottom, respectively). (D) Fluorescent responses of hsGFP (0.5 μM) to H<sub>2</sub>S at low micromolar concentrations.

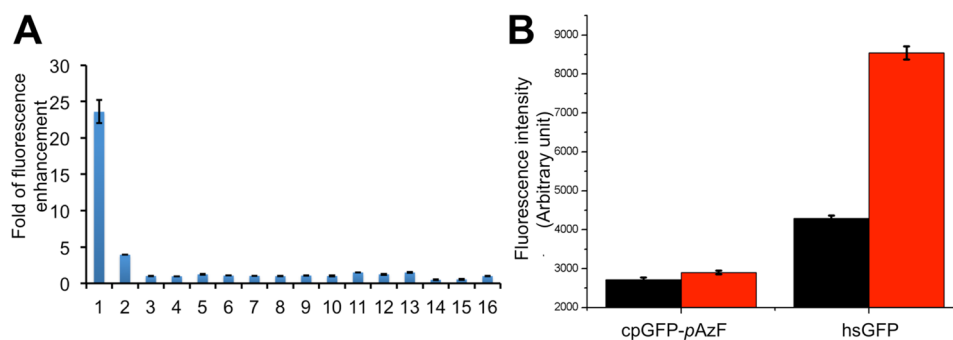


**Figure 4.** (A) Chemoselectivity of hsGFP against a panel of redox-active chemicals: (1) 1 mM H<sub>2</sub>S, (2) 100 μM H<sub>2</sub>S, (3) 1 mM H<sub>2</sub>O<sub>2</sub>, (4) 5 mM reduced glutathione, (5) 5 mM L-cysteine, (6) 100 μM HOCl, (7) 100 μM HOOtBu, (8) 100 μM O<sub>2</sub><sup>•−</sup>, (9) 20 μM ONOO<sup>−</sup>, (10) 100 μM NOC-7 (NO<sup>•</sup> donor), (11) 1 mM DTT, (12) 1 mM vitamin C, (13) 1 mM homocysteine, (14) •OH (1 mM Fe<sup>2+</sup> and 100 μM H<sub>2</sub>O<sub>2</sub>), (15) •OtBu (1 mM Fe<sup>2+</sup> and 100 μM HOOtBu), and (16) PBS. (B) Fluorescence intensities of *E. coli* cells expressing cpGFP-pAzF or hsGFP before (black) and after (red) reaction with 200 μM H<sub>2</sub>S.

criterion. Through this process, we identified a very promising mutant showing a >20-fold enhancement of fluorescence intensity in response to 1 mM H<sub>2</sub>S. We named it hsGFP and conducted further work to characterize it *in vitro* and in living cells.

**Spectroscopic Responses of hsGFP to H<sub>2</sub>S.** We examined the optical properties of hsGFP before and after

addition of H<sub>2</sub>S buffered in PBS (pH 7.4). The absorbance spectrum of hsGFP showed a major peak at 391 nm, corresponding to a *p*-azidobenzylideneimidazolidone chromophore (Figure 3A). After H<sub>2</sub>S had been added, the absorbance at 452 nm increased at the expense of the absorbance at 391 nm, indicating the formation of a new *p*-aminobenzylideneimidazolidone chromophore. Addition of H<sub>2</sub>S caused a dramatic

**Table 1. Fluorescence Properties of hsGFP and cpGFP-*pAzF***

	$H_2S$	$\lambda_{abs}$ (nm) with $\epsilon$ ( $M^{-1} cm^{-1}$ ) in parentheses	$\lambda_{em}$ (nm) with $\Phi$ in parentheses	brightness ( $M^{-1} cm^{-1}$ )	$x$ -fold intensity enhancement at the indicated $H_2S$ concentration	
					100 $\mu M$	1 mM
hsGFP	—	391 (66)	ND <sup>a</sup>	ND <sup>a</sup>	5.5	23
	+	452 (53)	500 (0.1)	5.3		
cpGFP- <i>pAzF</i>	—	375 (13)	ND <sup>a</sup>	ND <sup>a</sup>	0.6	1.5
	+	481 (20)	509 (0.03)	0.6		

<sup>a</sup>Not determined.

increase in the fluorescence excitation and emission signals (with peaks at 454 and 500 nm, respectively), suggesting that the reduced *p*-aminobenzylideneimidazolidone product is highly fluorescent (Figure 3B). The basal fluorescent signal before reaction was likely due to the background formation of a tyrosine-derived chromophore and the pre-reduction of an azide-derived chromophore to an amine-derived chromophore.

To determine the sensitivity of hsGFP to  $H_2S$ , we measured the fluorescence response of hsGFP to various concentrations of  $H_2S$ . We found that fluorescence changes were often completed within the first 20–30 min (Figure 3C). Upon incubation with 100  $\mu M$  or 1 mM  $H_2S$ , the green fluorescence of hsGFP increased by  $\sim 5.5$ - or 23-fold, respectively. Considering these large changes, we suspected that hsGFP could detect  $H_2S$  at low physiological concentrations. To test this, we measured the response of hsGFP to  $H_2S$  at low micromolar concentrations (Figure 3D). The limit of detection (LOD) was determined to be 435 nM, making hsGFP one of the most responsive fluorescent probes yet developed, for  $H_2S$  detection (Figure 3D).<sup>42</sup> Collectively, these data indicate that hsGFP is a robust and highly sensitive probe for  $H_2S$ .

Cells generate a variety of redox-active molecules under normal and stress conditions. To unambiguously detect  $H_2S$  in such a complex environment, fluorescent probes that are not responsive to other relevant redox-active molecules are required. To test the selectivity of hsGFP, we systematically measured its response to a range of redox-active molecules, including competing thiols, and reactive oxygen, nitrogen, and sulfur species, at physiologically relevant or higher concentrations (Figure 4A). Notably, except for  $H_2S$ , all other tested molecules triggered no or limited fluorescence responses, suggesting that hsGFP is a highly selective fluorescent probe toward  $H_2S$ .

**Comparison of hsGFP to cpGFP-*pAzF*.** Compared to the first-generation  $H_2S$  probe cpGFP-*pAzF*, the most striking improvement of hsGFP was its large fluorescence response. At 100  $\mu M$  and 1 mM  $H_2S$ , cpGFP-*pAzF* showed 0.6- and 1.5-fold fluorescence increases, respectively.<sup>34</sup> Therefore, the magnitudes of hsGFP fluorescence changes under the same conditions have improved by 920 and 1530%, respectively (Table 1). We utilized electrospray time-of-flight mass spectrometry (ESI-TOF MS) to characterize freshly purified hsGFP (Figure S1 of the Supporting Information). The major peak corresponded to a mature *p*-azidobenzylideneimidazolidone chromophore. In contrast, the main portion of freshly purified cpGFP-*pAzF* was the precursor peptide that does not undergo chromophore maturation reactions.<sup>34</sup> The improved folding and chromophore maturation, caused by superfolder mutations, may partially explain the differences in fluorescence responses, because a portion of  $H_2S$ -reacted cpGFP-*pAzF* may

be trapped in an intermediate state and not form the mature *p*-aminobenzylideneimidazolidone chromophore during the short period of fluorescence analysis. Furthermore, the postreaction product of hsGFP was also considerably more fluorescent. We characterized the extinction coefficients ( $\epsilon$ ) and quantum yields ( $\Phi$ ) of hsGFP and cpGFP containing *p*-aminophenylalanine (*pAmF*)-derived chromophores. hsGFP-*pAmF* is  $\sim 9$ -fold brighter than cpGFP-*pAmF* (Table 1). In addition, because the magnitudes of enhancement at the two concentrations were not identical, there were likely differences in reaction kinetics, as well. Additionally, the fluorescence excitation and emission peaks of hsGFP-*pAmF* were blue-shifted by  $\sim 29$  and  $\sim 9$  nm from the fluorescent peaks of cpGFP-*pAmF*, respectively. This was not surprising, because Phe203 of cpGFP can possibly induce a  $\pi$ -stacking interaction with the chromophore to shift the peaks toward the red end of the spectrum.<sup>43</sup>

We also directly compared hsGFP with cpGFP-*pAzF* in living *E. coli* cells (Figure 4B). Cells were cultured and induced for protein expression under the same conditions. Higher fluorescence intensities were observed for hsGFP than for cpGFP-*pAzF*, before and after  $H_2S$  treatment. After 200  $\mu M$   $H_2S$  had been added to the cells, the fluorescence of cpGFP-*pAzF*-expressing cells increased marginally, while the increase in the fluorescence of hsGFP-containing *E. coli* cells was dramatic. This result indicates that hsGFP can be highly expressed and is more responsive to  $H_2S$  than is cpGFP-*pAzF*.

It is interesting to note that, although the first-generation  $H_2S$  probe cpGFP-*pAzF* reacts more preferably with dithiothreitol (DTT), a common reducing reagent used in molecular biology, than with  $H_2S$ ,<sup>34</sup> hsGFP has a lower reactivity toward DTT than toward  $H_2S$  (Figure 4A). This phenomenon may be related to the tight packing of superfolder GFP, because DTT is a considerably larger molecule than  $H_2S$ . In addition, the evolved hsGFP has a proline and a tryptophan at its N- and C-termini, respectively. Previous work suggested a strong stabilizing interaction between proline and tryptophan.<sup>44</sup> Such interaction may also be important here, because it may help exclude the larger hydrophilic DTT molecules from the hsGFP chromophore. The data also support that the reactivity of a chemical functional group can be well-modulated by its environment. In our case, “the environment” is the circularly permuted fluorescent protein scaffold, and the chemoselectivity of the chromophore has shifted during directed protein evolution. Therefore, except for the ability to be genetically encoded, the unnatural fluorescent protein probes are advantageous in the sense that an effective method (i.e., directed protein evolution) is available to tune the reactivity and specificity of these fluorescent probes.

**Expression of hsGFP in Live Mammalian Cells and Subcellular Domains.** Having confirmed that hsGFP is a

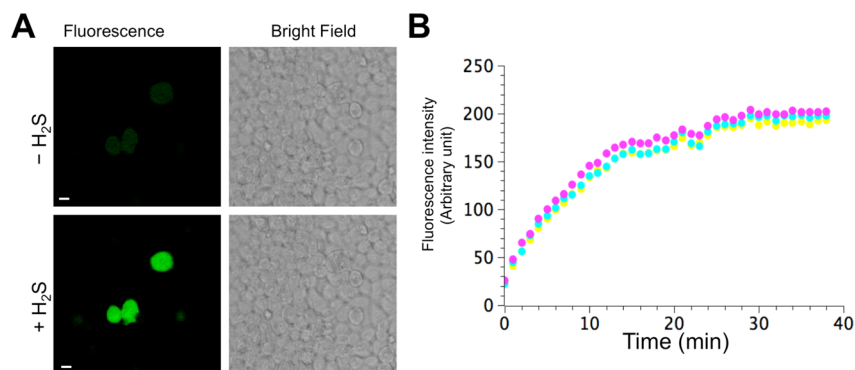


**Figure 5.** (A) Live fluorescence imaging of HEK 293T cells expressing hsGFP before and after addition of 50  $\mu$ M buffered H<sub>2</sub>S for 40 min. The scale bar is 50  $\mu$ m. (B) Quantified fluorescence intensities of individual fluorescent cells shown in panel A (top, magenta; bottom left, cyan; bottom right, yellow).

robust, sensitive, and selective fluorescent probe for the detection of H<sub>2</sub>S *in vitro*, we sought to explore its applications for imaging in live mammalian cells. Upon challenging transiently transfected hsGFP in HEK 293T cells with 50  $\mu$ M H<sub>2</sub>S, we observed a large increase in fluorescence (Figure 5A and the movie in the Supporting Information). We analyzed the time-dependent fluorescence change of single cells, and an ~8-fold fluorescence increase was observed (Figure 5B). Compared to *in vitro* assays, this higher magnitude of H<sub>2</sub>S-triggered fluorescence enhancement can be attributed to a better fidelity of pAzF incorporation and less preconversion of azide to amine in mammalian cells than in *E. coli*. The results demonstrate that hsGFP is highly responsive to H<sub>2</sub>S in living mammalian cells, consistent with our observations *in vitro* and in *E. coli* cells.

Fluorescent redox probes that can be localized to subcellular domains are particularly invaluable for measuring the dynamics of locally produced reactive molecules, such as H<sub>2</sub>S. To generate subcellular domain-associated H<sub>2</sub>S probes, we individually fused hsGFP to a mitochondrial targeting signal, a nuclear localization signal, or the Kir6.2 subunit of the K<sub>ATP</sub> channel. These constructs were expressed in HEK 293T cells. Upon treatment of these recombinant probes with H<sub>2</sub>S, we were able to confirm the localization of the recombinant hsGFP probes at the predicted subcellular locations (Figure 6), suggesting that hsGFP is a robust and versatile fluorescent probe that provides a convenient approach for future investigations of H<sub>2</sub>S signaling with subcellular resolution.

**Detection of Biologically Generated H<sub>2</sub>S.** After confirming the capacity of hsGFP to detect exogenous H<sub>2</sub>S, we next sought to determine whether hsGFP could detect enzymatically produced H<sub>2</sub>S in live mammalian cells. L-Cysteine, a nonessential amino acid and an important sulfide source in human metabolism, is a major precursor for the enzymatic production of H<sub>2</sub>S in mammals.<sup>4</sup> Endogenously, HEK 293T cells express H<sub>2</sub>S-generating enzymes such as CSE.<sup>45</sup> Upon stimulating hsGFP-expressing HEK 293T cells with 1 mM L-cysteine, we observed a prominent fluorescence enhancement, compared to the fluorescence of the negative control group that was not supplemented with L-cysteine (Figure 7). Furthermore, overexpressing an H<sub>2</sub>S-generating enzyme, CBS, in HEK 293T cells increased the basal fluorescence intensities of both L-cysteine-stimulated and unstimulated groups. HEK 293T cells that were overexpressing CBS and stimulated by L-cysteine showed a synergistic increase in fluorescence intensities versus those of groups that were singly either overexpressing CBS or stimulated by L-cysteine,

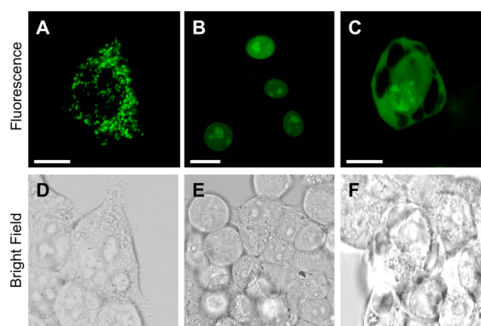


**Figure 6.** Localization of hsGFP to subcellular domains of HEK 293T cells. HEK 293T cells expressing hsGFP individually fused with either mitochondrial targeting signal, nuclear localization signal, or Kir6.2 subunit were treated with H<sub>2</sub>S, showing the localization of hsGFP to (A) the mitochondrial matrix and (B) cell nuclei or around (C) K<sub>ATP</sub> channels, respectively. (D–F) Corresponding bright field images of the cells in panels A–C, respectively. The scale bar is 50  $\mu$ m.

suggesting that CBS overexpression leads to a larger L-cysteine-induced fluorescence enhancement in hsGFP-expressing HEK 293T cells. We also quantified the fluorescence intensities of single cells, and significant differences were identified between groups with a two-tailed Student's *t* test (Figure 8). It is worth noting that the typical cell culture media contain ~0.3 mM L-cysteine, which may have contributed to the basal fluorescence. Nevertheless, the stimulation with 1 mM fresh L-cysteine was able to induce the production of additional H<sub>2</sub>S and trigger the fluorescence response of hsGFP. This experiment further confirmed that hsGFP is a highly responsive and selective H<sub>2</sub>S probe and can be utilized to detect H<sub>2</sub>S under biologically relevant conditions.

## CONCLUSION

By introducing pAzF into a new superfolder cpGFP template followed by fluorescence screening of a randomized library, we identified hsGFP as a dramatically enhanced, genetically encoded fluorescent probe for H<sub>2</sub>S. hsGFP has an unusually large response to H<sub>2</sub>S, allowing sensitive and selective detection of H<sub>2</sub>S, both *in vitro* and in living cells. Moreover, for the first time, we showed that hsGFP could be precisely localized to subcellular domains by creating genetic fusions with targeting signal peptides or other cellular proteins. Because this approach is general, it may be adapted to address the technical challenges of monitoring H<sub>2</sub>S at various subcellular locations. This method may also be utilized to deliver other similar fluorescent probes,



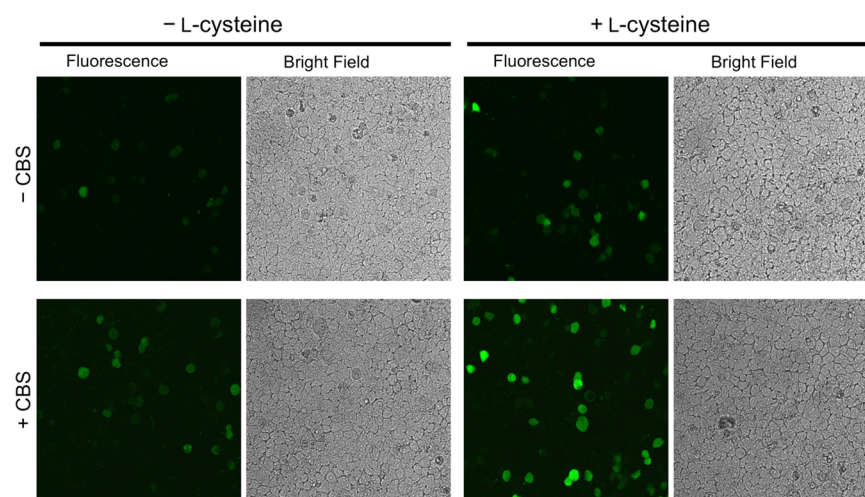


**Figure 7.** Response of hsGFP to L-cysteine in HEK 293T cells. Representative images of hsGFP expression in HEK 293T cells with (bottom row) or without (top row) CBS overexpression, in the absence (two left columns) or presence (two right columns) of 1 mM L-cysteine.

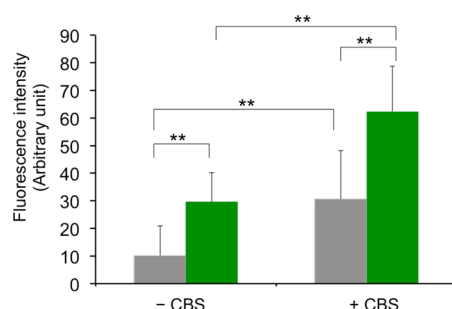


**Figure 8.** Average fluorescence intensities of individual hsGFP-expressing HEK 293T cells, with or without CBS overexpression, in the absence (gray) or presence (green) of 1 mM L-cysteine. Ten individual cells were analyzed for each group. Data are means  $\pm$  SD (\*\* $P < 0.01$ , from a two-tailed Student's *t* test).

such as the recently reported ONOO<sup>−</sup> probe, pnGFP.<sup>38</sup> Although various synthetic H<sub>2</sub>S probes have been developed, only a small percentage have been tested near physiological conditions. We performed fluorescence imaging of H<sub>2</sub>S production in HEK 293T cells stimulated with L-cysteine and showed that the fluorescence of hsGFP reflected the relative amount of enzymatically generated H<sub>2</sub>S in live cells. With these results, it is convincing that hsGFP is a highly robust fluorescent probe for H<sub>2</sub>S that has the potential to facilitate a broad spectrum of research on the biochemistry and cell biology of H<sub>2</sub>S signaling. Additionally, we expect that hsGFP may be used to develop fluorescent assays for screening inhibitors or activators of H<sub>2</sub>S-producing enzymes, potentially leading to important new pharmacological tools and drug candidates.

## ■ ASSOCIATED CONTENT

### ● Supporting Information

Sequences of oligonucleotides used in this study, ESI-TOF MS analysis of hsGFP, and a movie showing time-lapse fluorescence changes of hsGFP-expressing HEK 293T cells in response to H<sub>2</sub>S. This material is available free of charge via the Internet at <http://pubs.acs.org>.

## ■ AUTHOR INFORMATION

### Corresponding Author

\*E-mail: [huiwang.ai@ucr.edu](mailto:huiwang.ai@ucr.edu). Phone: (951) 827-3710.

### Funding

This work was supported by National Science Foundation Grant CHE-1351933 and the UCR Academic Senate Regents' Faculty Fellowship to H.-w.A.

### Notes

The authors declare no competing financial interest.

## ■ ACKNOWLEDGMENTS

We are grateful to Prof. Colin Nichols for providing plasmids pSUR1-EYFP and pcDNA3.1-Kir6.2-GFP and the DNASU plasmid repository for providing the CBS gene. We thank the UCR High Resolution Mass Spectrometry Facility for protein analysis.

## ■ ABBREVIATIONS

GFP, green fluorescent protein; cpGFP, circularly permuted GFP; UAA, unnatural amino acid; pAzF, *p*-azidophenylalanine; pAmF, *p*-aminophenylalanine; pBoF, *p*-boronophenylalanine; PCR, polymerase chain reaction; Ni-NTA, nickel-nitrilotriacetic acid; LB, Luria-Bertani; TB, terrific broth; K<sub>ATP</sub> channels, ATP-sensitive potassium channels; CBS, cystathionine  $\beta$ -synthase; CSE, cystathionine  $\gamma$ -lyase; 3-MST, 3-mercaptopyruvate sulfurtransferase; HEK, human embryonic kidney; BSA, bovine serum albumin; SUR1, sulfonylurea receptor 1; PBS, phosphate-buffered saline; LOD, limit of detection; DTT, dithiothreitol; ESI-TOF MS, electrospray time-of-flight mass spectrometry; SD, standard deviation.

## ■ REFERENCES

- (1) Reiffenstein, R. J., Hulbert, W. C., and Roth, S. H. (1992) Toxicology of hydrogen sulfide. *Annu. Rev. Pharmacol. Toxicol.* 32, 109–134.
- (2) Bates, M. N., Garrett, N., and Shoemack, P. (2002) Investigation of health effects of hydrogen sulfide from a geothermal source. *Arch. Environ. Health* 57, 405–411.
- (3) Muyzer, G., and Stams, A. J. (2008) The ecology and biotechnology of sulphate-reducing bacteria. *Nat. Rev. Microbiol.* 6, 441–454.

- (4) Li, L., Rose, P., and Moore, P. K. (2011) Hydrogen sulfide and cell signaling. *Annu. Rev. Pharmacol. Toxicol.* 51, 169–187.
- (5) Nishida, M., Sawa, T., Kitajima, N., Ono, K., Inoue, H., Ihara, H., Motohashi, H., Yamamoto, M., Suematsu, M., Kurose, H., van der Vliet, A., Freeman, B. A., Shibata, T., Uchida, K., Kumagai, Y., and Akaike, T. (2012) Hydrogen sulfide anion regulates redox signaling via electrophile sulfhydration. *Nat. Chem. Biol.* 8, 714–724.
- (6) Shatalin, K., Shatalina, E., Mironov, A., and Nudler, E. (2011) H<sub>2</sub>S: A universal defense against antibiotics in bacteria. *Science* 334, 986–990.
- (7) Wang, R. (2003) The gasotransmitter role of hydrogen sulfide. *Antioxid. Redox Signaling* 5, 493–501.
- (8) Mustafa, A. K., Gadalla, M. M., Sen, N., Kim, S., Mu, W., Gazi, S. K., Barrow, R. K., Yang, G., Wang, R., and Snyder, S. H. (2009) H<sub>2</sub>S signals through protein S-sulfhydration. *Sci. Signaling* 2, ra72.
- (9) Sen, N., Paul, B. D., Gadalla, M. M., Mustafa, A. K., Sen, T., Xu, R., Kim, S., and Snyder, S. H. (2012) Hydrogen sulfide-linked sulfhydration of NF- $\kappa$ B mediates its antiapoptotic actions. *Mol. Cell* 45, 13–24.
- (10) Wang, R. (2010) Hydrogen sulfide: The third gasotransmitter in biology and medicine. *Antioxid. Redox Signaling* 12, 1061–1064.
- (11) Wang, R. (2012) Physiological implications of hydrogen sulfide: A whiff exploration that blossomed. *Physiol. Rev.* 92, 791–896.
- (12) Yang, W., Yang, G., Jia, X., Wu, L., and Wang, R. (2005) Activation of K<sub>ATP</sub> channels by H<sub>2</sub>S in rat insulin-secreting cells and the underlying mechanisms. *J. Physiol.* 569, 519–531.
- (13) Eto, K., Asada, T., Arima, K., Makifuchi, T., and Kimura, H. (2002) Brain hydrogen sulfide is severely decreased in Alzheimer's disease. *Biochem. Biophys. Res. Commun.* 293, 1485–1488.
- (14) Kamoun, P., Belardinelli, M. C., Chabli, A., Lallouchi, K., and Chadeaux-Vekemans, B. (2003) Endogenous hydrogen sulfide overproduction in Down syndrome. *Am. J. Med. Genet. Part A* 116A, 310–311.
- (15) Wu, L., Yang, W., Jia, X., Yang, G., Duridanova, D., Cao, K., and Wang, R. (2009) Pancreatic islet overproduction of H<sub>2</sub>S and suppressed insulin release in Zucker diabetic rats. *Lab. Invest.* 89, 59–67.
- (16) Yang, G. D., Wu, L. Y., Jiang, B., Yang, W., Qi, J. S., Cao, K., Meng, Q. H., Mustafa, A. K., Mu, W. T., Zhang, S. M., Snyder, S. H., and Wang, R. (2008) H<sub>2</sub>S as a physiologic vasorelaxant: Hypertension in mice with deletion of cystathionine  $\gamma$ -lyase. *Science* 322, 587–590.
- (17) Fiorucci, S., Antonelli, E., Mencarelli, A., Orlandi, S., Renga, B., Rizzo, G., Distrutti, E., Shah, V., and Morelli, A. (2005) The third gas: H<sub>2</sub>S regulates perfusion pressure in both the isolated and perfused normal rat liver and in cirrhosis. *Hepatology* 42, 539–548.
- (18) Peng, H. J., Chen, W. X., Burroughs, S., and Wang, B. H. (2013) Recent advances in fluorescent probes for the detection of hydrogen sulfide. *Curr. Org. Chem.* 17, 641–653.
- (19) Xuan, W. M., Sheng, C. Q., Cao, Y. T., He, W. H., and Wang, W. (2012) Fluorescent probes for the detection of hydrogen sulfide in biological systems. *Angew. Chem., Int. Ed.* 51, 2282–2284.
- (20) Hou, F. P., Cheng, J., Xi, P. X., Chen, F. J., Huang, L., Xie, G. Q., Shi, Y. J., Liu, H. Y., Bai, D. C., and Zeng, Z. Z. (2012) Recognition of copper and hydrogen sulfide in vitro using a fluorescein derivative indicator. *Dalton Trans.* 41, 5799–5804.
- (21) Hou, F. P., Huang, L., Xi, P. X., Cheng, J., Zhao, X. F., Xie, G. Q., Shi, Y. J., Cheng, F. J., Yao, X. J., Bai, D. C., and Zeng, Z. Z. (2012) A retrievable and highly selective fluorescent probe for monitoring sulfide and imaging in living cells. *Inorg. Chem.* 51, 2454–2460.
- (22) Sasakura, K., Hanaoka, K., Shibuya, N., Mikami, Y., Kimura, Y., Komatsu, T., Ueno, T., Terai, T., Kimura, H., and Naganot, T. (2011) Development of a highly selective fluorescence probe for hydrogen sulfide. *J. Am. Chem. Soc.* 133, 18003–18005.
- (23) Liu, C., Pan, J., Li, S., Zhao, Y., Wu, L. Y., Berkman, C. E., Whorton, A. R., and Xian, M. (2011) Capture and visualization of hydrogen sulfide by a fluorescent probe. *Angew. Chem., Int. Ed.* 50, 10327–10329.
- (24) Liu, C. R., Peng, B., Li, S., Park, C. M., Whorton, A. R., and Xian, M. (2012) Reaction based fluorescent probes for hydrogen sulfide. *Org. Lett.* 14, 2184–2187.
- (25) Qian, Y., Karpus, J., Kabil, O., Zhang, S.-Y., Zhu, H.-L., Banerjee, R., Zhao, J., and He, C. (2011) Selective fluorescent probes for live-cell monitoring of sulphide. *Nat. Commun.* 2, 495.
- (26) Das, S. K., Lim, C. S., Yang, S. Y., Han, J. H., and Cho, B. R. (2012) A small molecule two-photon probe for hydrogen sulfide in live tissues. *Chem. Commun.* 48, 8395–8397.
- (27) Lippert, A. R., New, E. J., and Chang, C. J. (2011) Reaction-based fluorescent probes for selective imaging of hydrogen sulfide in living cells. *J. Am. Chem. Soc.* 133, 10078–10080.
- (28) Montoya, L. A., and Pluth, M. D. (2012) Selective turn-on fluorescent probes for imaging hydrogen sulfide in living cells. *Chem. Commun.* 48, 4767–4769.
- (29) Peng, H., Cheng, Y., Dai, C., King, A. L., Predmore, B. L., Lefer, D. J., and Wang, B. (2011) A fluorescent probe for fast and quantitative detection of hydrogen sulfide in blood. *Angew. Chem., Int. Ed.* 50, 9672–9675.
- (30) Yu, F. B. A., Li, P., Song, P., Wang, B. S., Zhao, J. Z., and Han, K. L. (2012) An ICT-based strategy to a colorimetric and ratiometric fluorescence probe for hydrogen sulfide in living cells. *Chem. Commun.* 48, 2852–2854.
- (31) Ren, W., and Ai, H. W. (2013) Genetically encoded fluorescent redox probes. *Sensors* 13, 15422–15433.
- (32) Chen, Y., Zhu, C., Yang, Z., Chen, J., He, Y., Jiao, Y., He, W., Qiu, L., Cen, J., and Guo, Z. (2013) A ratiometric fluorescent probe for rapid detection of hydrogen sulfide in mitochondria. *Angew. Chem., Int. Ed.* 52, 1688–1691.
- (33) Liu, T., Xu, Z., Spring, D. R., and Cui, J. (2013) A lysosome-targetable fluorescent probe for imaging hydrogen sulfide in living cells. *Org. Lett.* 15, 2310–2313.
- (34) Chen, S., Chen, Z. J., Ren, W., and Ai, H. W. (2012) Reaction-based genetically encoded fluorescent hydrogen sulfide sensors. *J. Am. Chem. Soc.* 134, 9589–9592.
- (35) Ai, H. W. (2012) Biochemical analysis with the expanded genetic lexicon. *Anal. Bioanal. Chem.* 403, 2089–2102.
- (36) Liu, C. C., and Schultz, P. G. (2010) Adding new chemistries to the genetic code. *Annu. Rev. Biochem.* 79, 413–444.
- (37) Makhina, E. N., and Nichols, C. G. (1998) Independent trafficking of K<sub>ATP</sub> channel subunits to the plasma membrane. *J. Biol. Chem.* 273, 3369–3374.
- (38) Chen, Z. J., Ren, W., Wright, Q. E., and Ai, H. W. (2013) Genetically encoded fluorescent probe for the selective detection of peroxynitrite. *J. Am. Chem. Soc.* 135, 14940–14943.
- (39) Chin, J. W., Santoro, S. W., Martin, A. B., King, D. S., Wang, L., and Schultz, P. G. (2002) Addition of *p*-azido-L-phenylalanine to the genetic code of *Escherichia coli*. *J. Am. Chem. Soc.* 124, 9026–9027.
- (40) Young, T. S., Ahmad, I., Yin, J. A., and Schultz, P. G. (2010) An enhanced system for unnatural amino acid mutagenesis in *E. coli*. *J. Mol. Biol.* 395, 361–374.
- (41) Pedelacq, J. D., Cabantous, S., Tran, T., Terwilliger, T. C., and Waldo, G. S. (2006) Engineering and characterization of a superfolder green fluorescent protein. *Nat. Biotechnol.* 24, 79–88.
- (42) Lin, V. S., Lippert, A. R., and Chang, C. J. (2013) Cell-trappable fluorescent probes for endogenous hydrogen sulfide signaling and imaging H<sub>2</sub>O<sub>2</sub>-dependent H<sub>2</sub>S production. *Proc. Natl. Acad. Sci. U.S.A.* 110, 7131–7135.
- (43) Wachter, R. M., Elsliger, M. A., Kallio, K., Hanson, G. T., and Remington, S. J. (1998) Structural basis of spectral shifts in the yellow-emission variants of green fluorescent protein. *Structure* 6, 1267–1277.
- (44) Biedermannova, L., E Riley, K., Berka, K., Hobza, P., and Vondrasek, J. (2008) Another role of proline: Stabilization interactions in proteins and protein complexes concerning proline and tryptophane. *Phys. Chem. Chem. Phys.* 10, 6350–6359.
- (45) Sekiguchi, F., Miyamoto, Y., Kanaoka, D., Ide, H., Yoshida, S., Ohkubo, T., and Kawabata, A. (2014) Endogenous and exogenous hydrogen sulfide facilitates T-type calcium channel currents in Cav3.2-



expressing HEK293 cells. *Biochem. Biophys. Res. Commun.* 445, 225–229.